Transient Lateral Transport of Platelet-Sized Particles in Flowing Blood Suspensions

Chinjung Yeh* and Eugene C. Eckstein‡
*Department of Biomedical Engineering, University of Miami; Miami, Florida; and ‡University of Tennessee, Memphis, Tennessee 38163 USA

ABSTRACT Concentration profiles of 2.5 μm latex beads were measured to demonstrate lateral transport of platelet-sized objects in flows of blood suspensions; the flows had equivalent Poiseuille wall shear rates (WSRs) from 250 to 1220 s^{-1}. Each experimental trial began with a steady flow of suspension without beads in a thin-walled capillary tube (219 μm ID; 10.2 μm SD). The tube entrance was then switched to a reservoir containing suspension of equal hematocrit, but with beads, for a short interval of flow at the same WSR. This process established a paraboloidal tongue of labeled suspension with a transient concentration gradient at its surface. The tube and contents were rapidly frozen to fix the suspended particles in flow-determined locations. Segments of frozen tube were collected at distances from the entrance corresponding to 13%, 39%, and 65% of the axial extent of the ideal paraboloidal tongue. Concentration profiles were estimated from distances measured on fluorescence microscope images of cross-cut tube segments. Experiments used tubes either 40 or 50 cm long, suspension hematocrits of 0, 15, or 40%, and bead concentrations in the range of 1.5–2.2 × $10^5/mm^3$. Profiles for 0% hematocrit suspension, a dilute, single-component suspension, had features expected in normal diffusive mixing in a flow. Distinctly different profiles and more lateral transport occurred when the suspensions contained red cells; then, all profiles for 13% extent had regions of excess bead concentration near the wall. Suspension flows with 40% hematocrit exhibited the largest amount of lateral transport. A case is made that, to a first approximation, the rate of lateral transport grew linearly with WSR; however, statistical analysis showed that for 40% hematocrit, less lateral transport occurred when the WSR was 250 s^{-1} or 1220 s^{-1} than 560 s^{-1}, thus indicating that the rate behavior is more complex.

INTRODUCTION

Experiments with flow-induced transient concentration gradients of platelet-sized latex beads were performed to demonstrate the concentration profiles associated with lateral transport in shearing blood suspensions. The expectation was that nondiffusive modes of transport would be revealed by features of the concentration profiles, e.g., by regions of elevated concentration. Controlled initial conditions were obtained by moving the entrance of a tube from a reservoir containing suspension without beads to one containing suspension with beads. The experiments resembled G. I. Taylor's classic studies of mixing tube flow; however, only the early phase of mixing was studied in our protocol. The mixing/dispersion in such experiments, often referred to as Taylor diffusion, is commonly analyzed with a convective diffusion equation, which may use an effective diffusion coefficient. (See Probstein (1989) for a lucid treatment of Taylor diffusion.) Turitto et al. (1972) used a similar method to deduce an effective diffusivity for platelets in flowing blood; they found that the range of wall shear rates (WSRs) for which they could use the Taylor method was limited, since anomalous lateral distribution of the platelets occurred when the WSR was over 440 s^{-1}. These experiments explore lateral transport at WSRs from 250 to 1220 s^{-1}; the concentration profiles shown below have local zones of elevated concentration that are not typical of diffusive transport and thus indicate that using a convective diffusive equation with an effective diffusion coefficient is inadequate. As noted near the end of the paper, these experiments are part of an effort to substantiate a model that uses a convective diffusion equation with an *ad hoc* drift term (Eckstein and Belgacem, 1991).

The parameters for the experiments were selected after reviewing previous experiments that demonstrated steady-state concentration profiles of platelet-sized latex beads in tube flows. Hematocrits of 15% and 40% were chosen because large near-wall excesses in concentrations profiles of platelet-sized beads were observed only when the hematocrit was significant, e.g., >10% (Tilles and Eckstein, 1987; Waters and Eckstein, 1990). Some experimental trials used suspensions without red cells (0% hematocrit). These were designated as "controls" to reflect that their solvent was Newtonian and "ideal" in the sense of modeling transport with a convective diffusion equation; they also met common conditions for being dilute. The comparison involves flows of platelet-sized beads in a simple solvent and flows of beads in a mixed solvent (red cells and suspending fluid). A one-component convective diffusion equation is traditionally used for a single species in a uniform solvent. For flowing blood suspensions, the region near the wall is known to exhibit relative separation of the mixed solvent, as illustrated by the marginal layer and its relative, the peripheral plasma layer; the applicable model is then an open question.

The lowest WSR was chosen as 250 s^{-1}, since significant near-wall excesses of platelet-sized latex beads were

Received for publication 27 September 1993 and in final form 2 February 1994.

Address reprint requests to Dr. Eugene C. Eckstein, Department of Biomedical Engineering, University of Tennessee, Memphis, 899 Madison Avenue, Suite 801, Memphis, TN 38163. Tel.: 901 448 7536; Fax: 901 448 7387; E-mail: eckstein@bme.utmem.edu.

0006-3495/94/05/1706/11 $2.00

observed only when the WSR was >200 s^{-1} (Tilles and Eckstein, 1987; Waters and Eckstein, 1990; Bilsker et al., 1989; Eckstein et al., 1988). Cavitation limited the largest WSR that could be studied to 1220 s^{-1}. As these values fell within typical ranges for the circulation and hollow-fiber artificial organs, the experimental data should be relevant to modelling platelet-surface interaction and the initial stages of thrombosis.

The discussion following the Results section places the data in a framework that aids in their interpretation, relates them to previous work, outlines likely causes for the nondiffusive transport, and builds a qualitative picture of platelet transport when nondiffusive effects are significant. Although no single cause of the nonuniform profiles is identified, reasons are provided for rejecting a hypothesis based upon shear-induced reduction of the available volume.

MATERIALS AND METHODS

Methods for the experiments parallelled those used to determine lateral concentration profiles in steady-state situations (Bilsker et al., 1989; Eckstein et al., 1989; Waters and Eckstein, 1990). In each trial, a tube conveying a suspension was rapidly frozen to capture the locations of fluorescent platelet-sized latex beads. Segments of the frozen tube at particular axial locations were collected and sectioned while frozen; the freshly exposed surfaces were viewed end-on with a fluorescence microscope, and the distances from each bead to the wall were measured. Radial concentration profiles were estimated from lists of the distance measurements. The text below further describes the methods; a complete account appears elsewhere (Yeh, 1991).

Suspensions

Blood suspensions were made with fresh human red cells that were washed three times in saline containing 0.5 wt/vol % human serum albumin (Fraction V, Sigma Chemical Co., St. Louis, MO). The suspending fluid was isotonic saline solution with 0.5 wt/vol % human serum albumin and 3.5 wt/vol % dextran 40 (Sigma). This dextran was selected to provide the effective viscosity of normal plasma, and because, with its moderate molecular weight, it had little tendency to bridge red cells and form rouleaux. Some suspensions included fluorescent tracer particles (2.5 μm diameter latex beads, Fluoresbrite, Polysciences, Warrington, PA) as platelet analogues; when beads were included, their number density was in the range of normal platelet counts (1.5–2.2 $\times$ 10^5/mm^3). The latex beads were exposed to albumin before being mixed with red cells; this was done to limit adhesion of beads to red cells. The interior wall of the polyethylene tube was stained with a fluorescent compound (Coumarin 7, Eastman, Rochester, NY) so it could be accurately located in the fluorescence images. To reduce adhesion of cells and beads, the tube wall was coated with albumin by exposure to an isotonic solution of saline and albumin (3.0 wt/vol %).

Freeze-capture method

During the flow portion of each trial, a syringe pump was connected to a horizontal polyethylene tube that continuously drew in suspension from a reservoir assembly. Groups of experimental trials were performed at selected values of the WSR in an equivalent Poiseuille flow, 8 U_{ave}/d, U_{ave} being the mean linear flow rate and d the tube diameter. The diameter of each tube was measured end-on with a microscope before the experimental trial. An appropriate flow rate for each trial was calculated using the measured diameter, the desired WSR, and the above formula. The tubes were 50 cm long for all trials except those with a WSR of 1220 s^{-1}. Tubes 40 cm long were used for those trials, since cavitation, and hence unreliable flow, occurred with longer tubes.

A reproducible transient concentration gradient was obtained by quickly sliding the tube entrance between reservoirs of suspension without and with beads while the pump ran. Both suspensions had the same hematocrit and were made with the same suspending fluid. An assembly consisting of a U-shaped channel that clamped two polyacrylate tubes among three rubber septa allowed changing the tube location without entry of air or obvious stoppage of flow. The parts were arranged to form two adjacent cylindrical reservoirs with puncturable end walls. To prevent mechanical damage to the polyethylene tube, its initial length was potted in hypodermic tubing; the tip of the polyethylene tube extended about 1 mm beyond the hypodermic tubing. The reservoir assembly was prepared for an experiment by first passing a piece of large-bore hollow needle through all three septa. The potted end of the polyethylene tube was slipped inside the needle so its potted portion passed through the reservoir that would be filled with suspension containing beads and the tube entrance was in the far reservoir. The needle was withdrawn while restraining the potted polyethylene tube so its entrance remained in the desired position.

At the beginning of an experimental trial, the tube was filled with saline containing albumin and the reservoirs were filled. (The reservoir containing the tip of the tube was filled with suspension without beads.) The syringe pump was set at the flow rate needed to produce the desired WSR and 30 min of withdrawal flow from the reservoir without beads occurred. Then the reservoir assembly was quickly pulled over the needle-potted tube so that the tube entrance moved into the reservoir containing suspension with beads. Use of soft, elastic septa prevented leakage around the needle-potted tube and avoided damage to the tip of the tube. The syringe pump was connected to the tube and operated at a constant withdrawal rate during the entire process. Times of flow of the second suspension were relatively short, ranging from 4 s for the highest WSR to 28 s for the lowest WSR. An electronic timer, which displayed time in tenths of seconds, was tripped when the tube was slipped between reservoirs. For most trials liquid nitrogen was manually dumped over the tube to freeze it at the desired time. To obtain accurate, short intervals of labeled flow for the trials at the highest WSR, a system composed of a delay circuit, an eccentrically hinged container of liquid nitrogen, and a solenoidal latch was used. Moving the needle-potted tube in the reservoir assembly triggered the delay circuit that, after the preset interval, retracted the solenoidal latch, which allowed gravity to tilt the container and flood liquid nitrogen over the tube.

Rapid freezing and the consequent formation of ice crystals of subcellular size were possible because the tubes had thin walls (~20 μm) and small total mass. The method of applying the liquid nitrogen was also an important concern. Gas is generated as a part of the cooling process, which during simple immersion tends to accumulate on surfaces and form an insulating layer. All trials used a flooding of liquid nitrogen over the tube, which swept away the gas generated in the cooling process. Inspection of images of sectioned tubes showed no ice crystals or unusual arrangements of cells or beads, thus indicating that ice crystallization occurred only at scales smaller than could be visualized with the microscope. Also, had significant rearrangement occurred, the control experiments would have produced unexpected results.

Axial locations for tube segments

To obtain concentration profiles from locations that exhibited lateral transport at various radial locations, centimeter-long segments of frozen tube were collected at axial locations that were 13, 39, and 65% of the total extent of travel of the ideal paraboloid. The extent of travel was calculated assuming that the suspensions did not mix and behaved as perfect Newtonian fluids; it equaled the product of the maximum velocity and the time of flow of suspension containing beads. The extent of travel was given by the expression $8\,Qt_{flow}/\pi d^2 = 2\,U_{ave}t_{flow}$, where the variables are flow rate, Q, time of labeled flow, t_{flow}, and tube diameter, d.

A secondary benefit of choosing segment locations at selected percentages of the extent of travel was that the locations were cast in a nondimensional form that adjusted for slight differences in the values of t_{inflow}. Cross-sectional planes at these axial locations intersected the ideal paraboloid at 93, 78, and 59% of the tube radius.

Image collection and concentration profiles

Tube segments were stored in liquid nitrogen until they could be sectioned for imaging the beads. The process for imaging surfaces of an individual segment began with embedding it in a cryomicrotome on the microscope stage. The tube was embedded so its circular end could be viewed through a fluorescence microscope (Nikon Labophot, 20× Fluor objective (NA 0.75), a 1-X video transfer lens in a trinocular eyepiece, and a body-factor magnification of 1.25 associated with the epifluorescence illuminator (FITC fluorescence filter set), and a video camera (Dage/MTI model PA-70). During the imaging process thin slices of the frozen tube segment were cut away with a cold knife and discarded. After each cut, the surface of the part of the segment remaining in the microtome was brought into focus and a digital image was collected using a DataTranslation frame-grabber board, an IBM-compatible computer, and a modular, custom program (Kippenhan, 1987). Images were collected quickly to avoid loss of detail due to frost accumulation. On occasion, freshly cut surfaces were rough and impossible to visualize; also, a few entire tube segments were lost, usually due to problems with embedding, sectioning, or warming of the cryomicrotome.

To analyze an image, the computer operator traced the position of the wall with a mouse and started a program module that located the bright pixels corresponding to platelet-sized fluorescent latex beads. As a check on the operation of the particle-locating module, the operator compared the original and computer-reduced images and, if differences were found, edited the image manually. Other modules made corrections for differences in video magnification in the vertical and horizontal directions, computed the least distance from each bead to the wall and wrote the distance to a file. Files containing distances from individual cross-sectional surfaces of the segment were grouped to form lists of distances. To estimate a radial probability density distribution for the beads, a list of distances was fed as raw data to a program that used a kernel-estimate technique involving fast Fourier transforms (Kippenhan, 1987; Silverman, 1986). Concentration profiles were obtained directly by transformation, since at a given radius, r, the concentration, $c(r)$, and the radial probability density, $p(r)$, are interrelated as $c(r) \sim p(r)/r$.

No suitable method was found to normalize the concentration profiles with respect to the reservoir concentration. In previous work with steady-state situations, concentration profiles were scaled to the reservoir concentration through the use of a mass-balance equation. That approach could not be transferred to the transient experiments because there was no way to account for the mass accumulation (a transient event) in the region of the tube between the entrance plane and the profile plane. Methods based on physical measurements of the reservoir concentration were stymied by the need to convert the image-based estimates of the number of particles per area to a concentration (particles per volume). Such conversions required methods to determine the thicknesses of the volumes in which bead images were counted. Due to the numerical aperture of the objective, only fluorescent beads in the uppermost few microns of the remaining tube segment appeared in images; however, no acceptable means to quantify this depth was found. Accordingly, profiles from the transient data were left in terms of number density profile (number of platelets/μ^2 of image). Although the dimensions are unusual (concentration as a number/area), the profiles have the same shape as profiles of true concentration (number/volume) or profiles that are normalized to the reservoir concentration, since all are interrelated by (unknown) multiplicative factors.

Segment-based average profile

Two different average concentration profiles can be calculated from the raw data for a set of experimental trials having the same parameters of hematocrit, WSR, and axial location of the tube segment. One method of data reduction lumps all bead-wall distance measurements from all images of the segments of all trials into a single list and uses the process described above to estimate a radial concentration profile. In this method, segments that have larger numbers of distance measurements will have a greater influence on the shape of the average concentration profile than segments with lesser numbers of distance measurements. In the other method, which was used for the profiles shown in Figs. 2 and 3, estimates of the concentration profiles for the individual segments were obtained first, and then an average of the several profiles was calculated. In this way, each segment was treated as having an equal amount of information; hence, the averages were termed "segment-based."

The process for calculating the segment-based average included steps to minimize effects associated with slight differences of tube diameter in a set of trials. The first step in calculating a segment-based average was to normalize the radial positions for the cumulative probability curves for each segment. The radius for any particular tube segment was taken as the average radius measured from all the images collected for that segment. Next, values of the cumulative probability density for each individual profile (segment) were obtained by interpolation at 200 equally spaced locations extending from the wall to the center. An average curve of cumulative probability density was calculated, and the segment-averaged concentration profile was calculated using the same method that was used for concentration profiles for individual segments.

A rationale for choosing the segment-based averages came from comparing the concentration profile based on all available distance measurements for a single tube segment (a best estimate profile) with concentration profiles based on subsets of the distance measurements for the same tube segment (lesser estimate profiles). Subsets were formed by selecting some group of images for the particular segment and using all measurements in the images. Choosing subsets of all the bead-wall measurements in this way mimicked the actual data collection process, since measurements were collected for all points observed on a cross-sectional plane. It also avoided issues related to making fair choices from the distance measurements for an individual image.

Visual inspection of profiles for individual segments showed that both the best and lesser estimates portrayed the basic features (e.g., the location and apparent width of a peak or its relative height) if the lesser estimates were made using some minimum number of particle-to-wall distance measurements. About 400 bead-wall measurements were necessary to provide a good representation of the profile when the beads were present over most of the tube cross-section. (Note that the value of profiles determined from larger numbers of measurements was not diminished by this observation, since they had an overall smoother appearance of the concentration profile and better definition of concentration gradients.) Importantly, comparing best estimates of profiles from different segments showed that the segments had features with different amplitudes. (The width of the near-wall peak was an exception; it varied relatively little among the profiles with obvious near-wall peaks.) On this basis, the segments were judged to contain independent amplitude information that would be carried into the segment-based average profile. To provide a sense of the variation in a typical set of trials, profiles for individual segments and the segment-based average curve are shown in Fig. 1. Estimates of the concentration profiles from 80 μm to the center were suppressed because they were highly erratic. Profiles for all trials are available from the corresponding author.

Cumulative probability density

It was useful to condense the information about bead distributions in the segments for a particular condition (WSR, hematocrit, and axial location) to a single representation. An obvious measure of lateral transport at various axial locations was provided by the number of beads that were outside the ideal paraboloid of labeled suspension that would have occurred if there were no mixing. In a more general sense, the number of beads found in an annulus bounded by the inner surface of the tube wall and a circle at some radial location provided a quantitative measure of the transport. Because different numbers of beads were observed in different segments, this measure was normalized by dividing the total number of beads observed in the segment. When this measure of transport was generated for each possible distance from the wall, the set of values was equivalent to a common statistic, the cumulative probability density function (CPDF).

The CPDF, especially as compared to estimates of the concentration, was robust in the sense that errors in the distance measurements did not strongly affect its value. The robust property of the CPDF stemmed from classifying particles as being on one side or the other of a boundary. Importantly, the error in the value of the CPDF was set by the *net* count of erroneous clas-

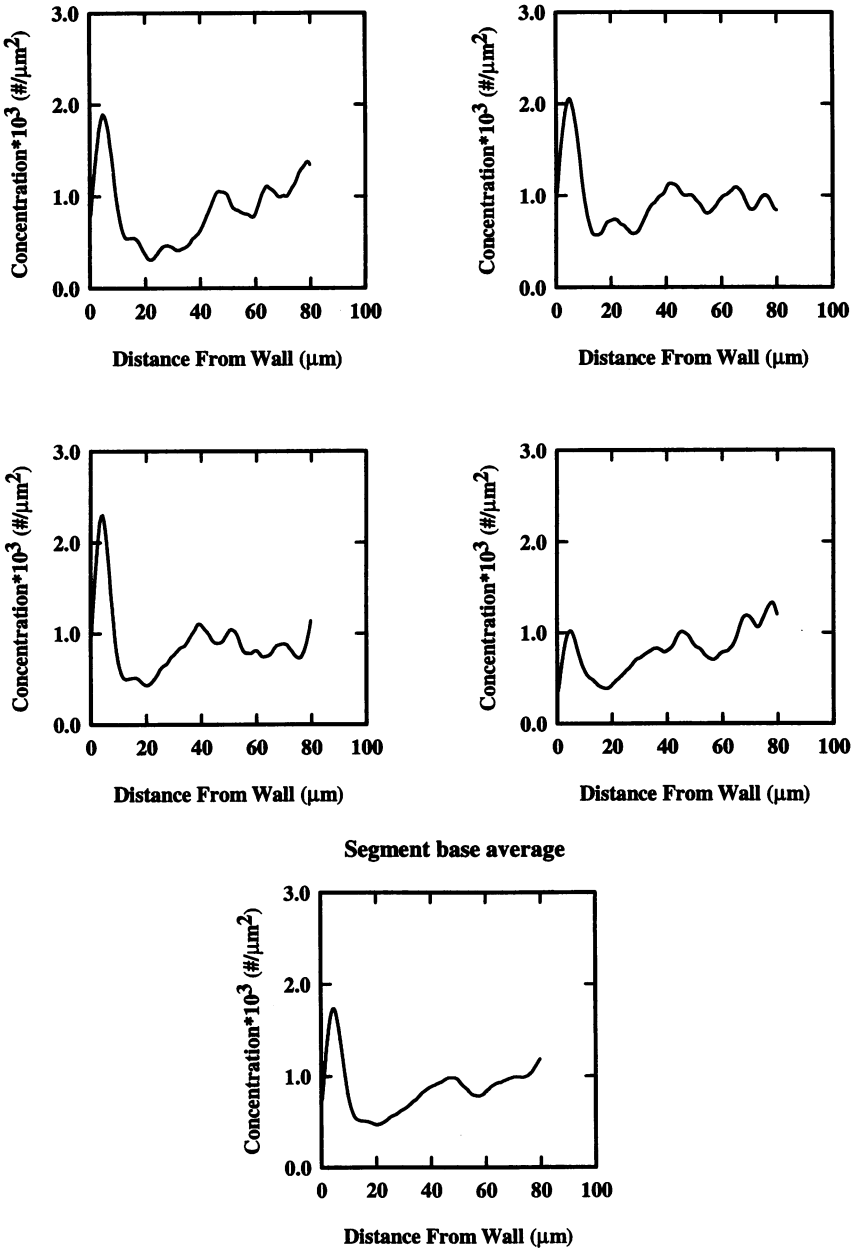

FIGURE 1 Concentration profiles from 13%-extent segments in trials with a hematocrit of 40% and a WSR of 560 s^{-1}. The upper four graphs show the profiles for segments from four separate trials and the lowest panel shows the segment-based average profile.

sifications of position with respect to the border. Except for locations very close to the wall, an individual particle position measurement produced a very small percentage change of the fraction of particles that are on one side of the boundary.

The shape of the CPDF provided much information about the concentration profile and the amount of lateral transport. For example, consider the ideal case of no lateral transport: the value of the CPDF would be 0 for all locations from the wall to the surface of the ideal paraboloid; over the range of positions from the surface to the center of the paraboloid, the CPDF would grow monotonically from 0 toward 1. The slope of the CPDF would decrease at positions closer to the center, since the circular geometry is associated with lesser total amounts of material in the central region. Lateral transport across the surface of the ideal paraboloid would reduce the size of the zone adjacent to the wall in which the CPDF equalled 0, and concomitantly, increase the value of the CPDF at the edge of the ideal paraboloid. When there was a near-wall peak, the CPDF in the near-wall region was concave downward. (This diagnostic was used only near the wall because in the center of the tube, the circular geometry and the relatively uniform concentration also produced a concave downward shape of the CPDF.)

Statistical design

Two sets of trials were run: one in a restricted range of WSR (520–560 s^{-1}) with three hematocrits (0, 15, and 40%) and the other at 40% hematocrit with four WSRs (250, 560, 800, and 1220 s^{-1}). All trials yielded profiles for at least two axial locations; sufficient trials were run so there were at least two concentration profiles for each axial location for each condition of the sets. Mean tube diameter for all trails was 219 μm (10.2 μm SD).

The null hypothesis for each set of trials was that the principal varied parameter, the hematocrit or WSR, did not change the amount of lateral transport. The null hypotheses were tested using a two-way ANOVA test in the statistical package, SigmaStat (Jandel Scientific, San Rafael, CA). The primary factor of interest was selected as either the hematocrit or the WSR. The second factor was selected as the axial position of the tube segment (extent). The amounts of lateral transport at the three axial locations (13, 39 and 65% extents) were considered to be independent measurements. The value of the CPDF at the off-wall location corresponding to the edge of the ideal paraboloid for the particular extent was used as a raw measure of lateral transport. The ANOVA computations passed the tests for normality and

equal variance provided in SigmaStat. After significant differences in factors were found, Student-Newman-Keuls tests were used for pairwise comparisons of the levels of the factors.

RESULTS

Hematocrit study

Inspection of Fig. 2 shows that the character of the segment-based average concentration profiles depended upon whether the suspensions contained red cells. The WSR for the left and center panels of Fig. 2 was 520 s^{-1}; that for the right panel was 560 s^{-1}. In the upper left panel, which shows concentration profiles for 0% hematocrit, each concentration profile has a gradient that rises to a region of approximately constant concentration. The irregularity ("bumpiness") in the region of approximately constant concentration, e.g., in the trace for 13% extent, the region extending from about 20 to 80 μm, reflects the limits of estimating a concentration profile from a small number of fluorescent beads observed in the sectioned segments. Smoother estimates could be obtained by using a wider kernel function in the kernel-estimate technique, but only at the cost of a less accurate depiction the concentration gradient (Silverman, 1986; Kippenhan, 1987). Clearly, the segments taken at greater distances from the tube entrance have greater distances between the wall and the steep, central portion of the gradient rising to the central concentration. The above points are shown more clearly by the CPDF curves, which owing to their integral nature, have less irregularity than the corresponding concentration profiles. Each CPDF curve begins to have significant non-zero values at an off-wall location that corresponds to the edge of the paraboloid. Also, the wall region of each CPDF is concave upward, indicating that no local peak or excess occurred near the wall.

Profiles for suspensions with 15% hematocrit are shown in the central panels of Fig. 2. The average concentration profile for the 13% extent segment has a significant peak, a fact that is confirmed by the concave downward shape of the near-wall portion of the corresponding CPDF. Comparing curves in the panels for 0% and 15% hematocrit by examining either the near-wall portions of the concentration profiles or the values of the CPDF at various radial locations shows that greater amounts of lateral bead transport occurs in red cell suspensions; this result is found for all three axial locations. A similar comparison of the panels for 15% and 40% hematocrit indicates that lateral transport is greater for 40% hematocrit: profiles for segments located at both 13% and 39% extent have near-wall excesses and the strength of lateral transport is great enough so that the segment at 65% extent (dotted line) exhibits material being transported all the way to the wall. In all cases, the CPDFs verify features noted in the profiles.

Statistical testing (ANOVA) indicated that after allowing for the effects of differences due to the position of the tube segment (i.e, the extent), the amount of lateral transport for the three hematocrits was significantly different ($p = 0.002$). The differences of mean values at various extents were also significantly different ($p = 0.014$). Subtesting for various levels of hematocrit indicated that the pairs, 40% vs. 0%, and 15% vs. 0% were significantly different at $p < 0.05$. Pairwise tests for the extents showed that 65% vs. 13% and 65% vs. 39% were different at $p < 0.05$. These findings for the value of the CPDF at the edge of the ideal paraboloid at the three axial locations paralleled features in the individual profiles; e.g., all profiles for the 13% extent segments for suspension hematocrits of 15% and 40% had near-wall peaks, while no profile there for 0% hematocrit has a near-wall excess.

Shear rate study

Profiles in Fig. 3 display the average outcome at various WSRs for the short-term transient transport of suspensions of 40% hematocrit in tubes of ~220 μm. At all shear rates, profiles for the segments at 13% extent had near-wall peaks.

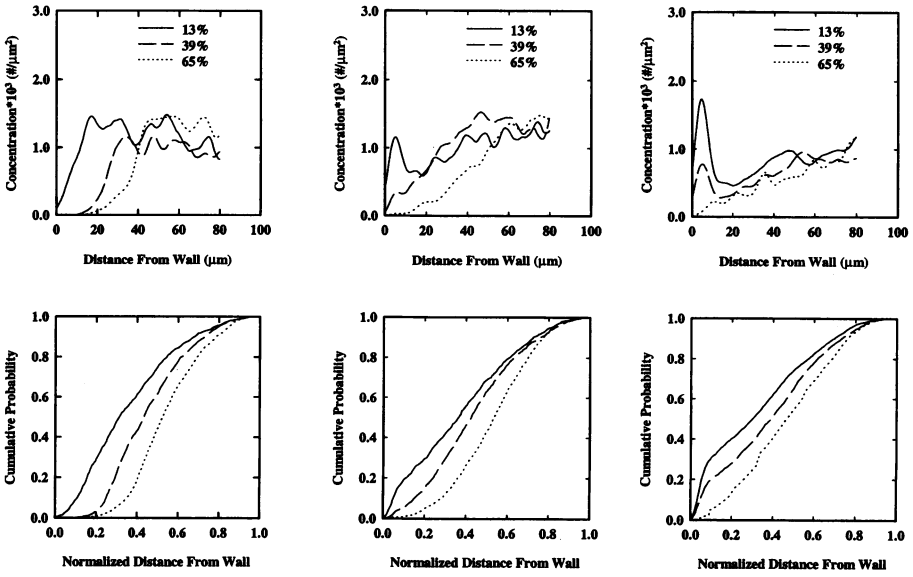

FIGURE 2 Segment-based average profiles for various suspension hematocrits. The upper graphs are concentration profiles and the lower graphs are cumulative probability distribution functions. Graphs at the left are for suspensions of 0% hematocrit; graphs at center are for suspensions of 15% hematocrit; graphs at the right are for suspensions of 40% hematocrit; WSRs are listed in the text.

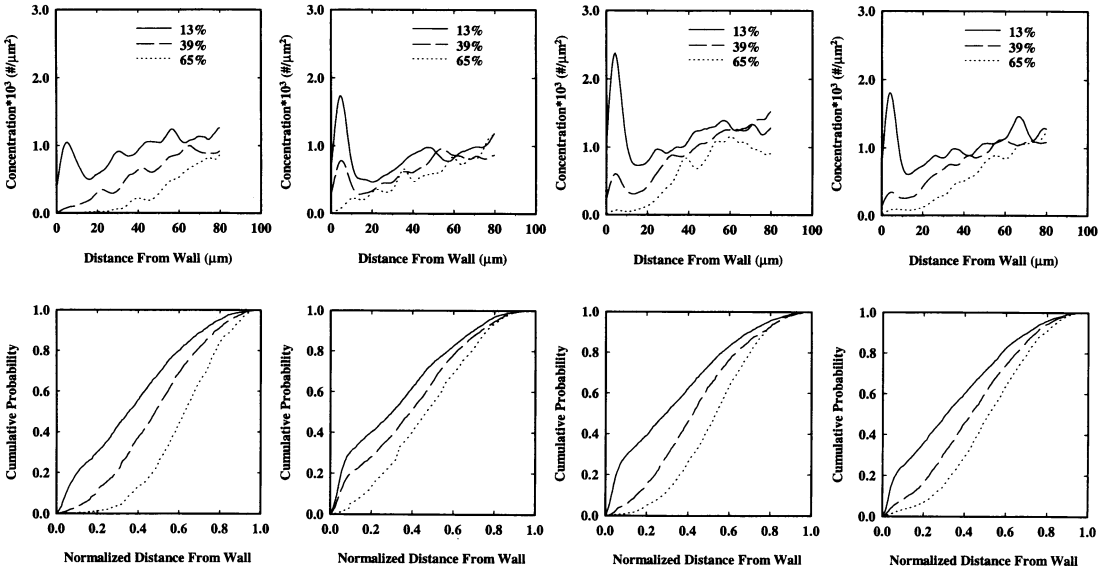

FIGURE 3 Segment-based average profiles for various WSRs. The arrangement of panels is similar to Fig. 2, but here suspension hematocrit is fixed at 40% and the WSR is varied. For the vertical pairs of graphs, the WSR values are (left to right): 250, 560, 800, 1220 s^{-1}.

For shear rates of 560, 800, and 1220 s^{-1}, near-wall peaks also occurred in profiles for the segments at 30% extent. Inspection of the near-wall portion of the 65%-extent profiles for higher WSRs shows that transport in this region occurred with very little gradient, an indication of a transport mode that differs from pure diffusion. This observation was supported by the nearly linear near-wall portion of the segmental average CPDFs for 65%-extent segments for the higher WSRs. The existence of near-wall peaks was reiterated in the shapes of the CPDFs.

The ANOVA test indicated that the differences in the mean amounts of lateral transport for various WSRs were significantly different with a p value of 0.001. In subsequent pairwise testing, lateral transport at the WSR of 560 s^{-1} was found to be significantly different from lateral transport at WSRs of 250 s^{-1} and 1220 s^{-1}, each with $p < 0.05$. Other pairwise comparisons were either not significant or fell into the "do-not-test" category.

DISCUSSION

Deductions based on the profiles for 0% hematocrit, i.e., the control experiments, led to the conclusion that experimental artifacts were not the cause of the profiles observed with the freeze-capture technique. Their shape was consistent with a small amount of diffusive smearing of the surface of the inflow paraboloid predicted by classical fluid mechanics. Since the experimental technique, including the freezing and sectioning steps, yielded expected shapes of profiles for 0% hematocrit, it was deemed capable of providing true profiles for other conditions. This view was solidified by the finding of increased lateral transport when red cells were present in the suspension flow, a finding that echoes much previous work (Turitto et al., 1972; Goldsmith, 1971; Goldsmith and Turitto, 1986). Importantly, the experimental technique provided a form of data, concentration profiles, that allows strong tests of models of lateral transport.

Idealizations

The type and nature of transport demonstrated by the experiments are revealed by comparing the experimental results to ideal motions in a well defined geometry. Several idealizations deserve mention. Inflow of the second suspension would form a paraboloidal tongue inside the tube for a purely convective flow (i.e., one without diffusion or mixing). The concentration profiles shown above are estimated from segments of tube that comprise about 2% of the total extent of travel of the ideal paraboloid. This distance is short enough that the profiles can be idealized as representing events on planes that perpendicularly intersect the paraboloid and tube axes at various positions. Without lateral transport, beads would only be found inside a circular region defined by the intersection of the plane and the paraboloid; this situation has the maximum possible gradient for lateral transport. The Peclet number, which provides a relative measure of convective to diffusive motions, is of order 10^6, a value that justifies ignoring bulk diffusive motion as compared to convective motion. Reflecting the limits of the short time of flow and the large Peclet number, the major determinant of outcome at any axial location is the convection, or equivalently, the major events take place in a zone surrounding the surface of the tongue of labeled suspension that flows into the tube.

An important idealization was that the suspension-related events were equivalent in both stages of flow. Although platelet-sized latex tracer beads were absent from one suspension and present in the other, the beads were individually small and comprised less than 0.2% of the volume of the total suspension. Since such a small component would exert a negligible influence on the suspension flow, the suspensions

were considered to have equal properties of viscosity and augmented diffusion coefficient. Each of these properties was strongly dependent on the suspension hematocrit. During the flow of the suspension without beads, statistically steady distributions of red cells and motions should be established in the tube. The quick changing of reservoirs allowed the feed suspension to be modified without altering the situation in the tube. There were no significant issues related to removing priming solutions or other dramatically different fluids. Thus, both stages of flow had statistically equal spatial distributions of red cells. Also, the hematocrit gradient that exists at the onset of flow of the suspension with beads is statistically equivalent to those present at the time of freezing in previous studies of the bead concentration in steady-state tube flows.

The lengths associated with development of velocity and hematocrit profiles were of interest since, for reasons noted below, the lateral transport involved shear-induced interaction of beads and red cells. Using the largest tube-based Reynolds number, which was ~10, and assuming the bulk suspension behaved like a Newtonian fluid, the velocity entrance length, was one tube diameter or less. Even though the discrete nature of red cells in a high shear-rate suspension flow led to different behavior than a similar flow of Newtonian fluid, it was probably a good estimate of the distance from the entrance that is required to develop a linear profile of shear stress (from a maximum value at the wall to 0 at the center). Redistribution of red cells over an unknown but longer length led to steady-state profiles of local viscosity, red cell concentration, and velocity. A subsidiary idealization involved separating the development of the marginal layer into similar lengths. It seemed reasonable to assume that mechanical exclusion and other strong local forces establish a "basic" marginal layer in about the same axial length that was required for the development of the profile of shear stress (about one tube diameter). Further development of the marginal layer, e.g., increasing its height or establishing a significant peripheral plasma layer, was then modeled as a part of development of the overall hematocrit profile. From these estimates, the velocity profile in the vast majority of the tube was quasi-parabolic. The near-wall zone where the peaks were observed was considered to be a well-sheared region with a predominantly lateral gradient of hematocrit.

Path-based inferences

Interesting points stem from the limits on possible paths that end in the sampled annular region outside the parabolic tongue. These points are based on the concept that because viscous forces dominate, the particle/bead always moves at close to the local convective velocity. This is the case when the particle Reynolds number (given by the expression $a^2\gamma/\nu$, where a = the particle radius, γ = the WSR, and ν = the kinematic viscosity) is much less than 1; the largest value in the experiments was 0.005.

The convective speeds associated with all the radial positions in the annular region at the axial sampling point are too small to carry a bead to that axial position in the time during which the second suspension flowed. This fact is true whether or not lateral transport occurs. Beads in the annular region must have spent some of their trip at the slower axial velocities; to reach the final position, other parts of the path must have involved faster velocities, which occurred inside the circle defined by the axial sectioning plane intersecting the paraboloid. This balance is particularly restrictive for the near-wall beads found in the segments at 65% of the final extent of the paraboloid. On the portions of the bead's path that were near the tube wall, it had small velocities, which were accommodated for by other portions of the path that had relatively large velocities. To obtain these faster velocities and to end near the wall, the bead had to undergo relatively large changes of radial position. The relatively small portion of the particles that make this type of journey is an indication of the basic dispersive character of lateral transport. A simple convective motion would not lead to such outcomes because it would move all the beads from some region on the same path. However, some fraction of the particles in a region could have large lateral motions if a directed, nondiffusive motion (such as a drift) supplemented a diffusive motion.

The distribution of beads in the inner portion of the paraboloid, i.e., the central part of the circular region, is best shown by the CPDF profiles, which appear in the lower panels of Figs. 2 and 3. Inspection of the profiles shows that the beads were evenly distributed in the inner parts of the paraboloid; all the CPDF profiles exhibit the characteristic concave downward shape that occurs for uniform concentration in the central region of a tube. Had the beads been systematically excluded from a core region, e.g., due to accumulation of red cells in that region, or if the concentration profiles there had local excesses or deficits, the CPDF profiles would have more complex shapes in the central region of the tube.

Observations stemming from transient and steady-state experiments

The nature of flow-induced lateral transport is clarified by joining observations from past studies with the above data. In previous studies tube segments were collected after there had been a steady flow of suspension with beads from a single reservoir for a long period (>20 min). The finding of indistinguishable profiles in experimental trials that involved shorter and longer intervals of flow before freezing indicated that a steady-state distribution of particles had occurred. Some studies collected profiles from various axial locations along the tube. The profiles determined from tube segments consisting of the first half centimeter had near-wall peaks that were less than twice the central concentration, whereas profiles from segments 2 or more cm downstream had near-wall peaks that were 4 to 10 times the central concentration (Waters and Eckstein, 1990). In this transient study the tube segments closest to the entrance (13% extent) were ~5 cm from the entrance; the near-wall peaks in them were almost always less than twice the central concentration. In combi-

nation, the observations indicate that the amount of transport demonstrated in these transient experiments is relatively small compared to the total amount needed to build a large scale near-wall peak in the concentration profile. Equally important, the combination demonstrates that events at the tube entrance (entrance effects) are not the primary source of the observed near-wall peaks in the concentration profiles. Specifically, there is no evidence that large-scale separation of beads and red cells occurs in the short entrance region at the tube inlet where the linear profile of shear stress is established, where there are associated acceleration, deceleration, and radial velocity fields, and where the initial distribution of red cells and the marginal layer are established.

Other steady-state studies examined the role of hematocrit (Eckstein et al., 1989). They showed that flows of suspensions of high hematocrits (60 and 80%) had smaller near-wall peaks than those of intermediate hematocrit (40%). The bead distributions observed in those experiments were, like these, approximately uniform in the central region of the tube, thus providing no indication of exclusion from the region expected to have the highest hematocrit.

Strain and rate of transport

The fact that relatively large amounts of transport were observed for the 40%-hematocrit trials at various WSRs (see Fig. 3) makes it desirable to characterize the rate of transport in an approximate way. Since the experimental trials involved approximately equal lengths of inflow of labeled blood suspension into the tube, the lateral transport was associated with a fixed amount of strain. For the higher WSR data, this implies that the amount of lateral transport was set by the totality of kinematic motions induced by the shearing flow (tumbling, passing of cells, etc.). To a first approximation, it follows that the rate of transport was proportional to the WSR, since the similar amounts of lateral transport occurred in progressively less times for higher values of WSR. The shear-rate dependent behavior of red cells has been well noted (Goldsmith and Turitto, 1986; Schmid-Schoenbein and Wells, 1969; Chien, 1975); it seems reasonable to postulate that red cell behavior governs the kinematic motions that lead to lateral transport. The statistically significant, relatively larger amount of lateral transport that occurred for 560 s^{-1} implies a special behavior at an intermediate range of WSR. This finding parallels an earlier one for steady flow of blood through capillary tubes of similar size and composition (Corattiyl and Eckstein, 1986); there, the ratio of tubular platelet concentration to reservoir platelet concentration was larger for the WSR of 800 s^{-1} than for values of 400 s^{-1} or 4000 s^{-1}.

Overview of transport processes in tube flows of blood

These results are consistent with classical concepts of microrheology, i.e., that the shearing action in a tubular suspension flow forces particles to interact continuously and that such interactions lead to lateral motions. The increased lateral transport for suspensions with 15% and 40% hematocrit, as compared to that at 0% hematocrit, is attributable to the much greater number of particles (red blood cells) in the suspension, which leads to both increased numbers of interactions and an increased likelihood of net lateral displacement after an interaction. Goldsmith showed that the shear-induced lateral displacements of individual platelet-sized latex beads and red cells in blood suspensions appeared to be erratic; he condensed the information in the record of particle position to a diffusion coefficient (Goldsmith, 1971). Judging the accuracy with which a diffusion coefficient represents a short record of lateral position is a very difficult task. The particle-position histories must be shown to be truly random, but very long records of particle position are required to demonstrate this property. For particles in suspension flows, the great practical difficulty of the experiments makes such records nearly impossible to obtain. Work by Turitto et al. (1972), who estimated diffusion coefficients for platelets, provides a practical demonstration of the utility of the diffusion model. For low WSRs, their results compare well with Goldsmith's estimates of the diffusion coefficient. However, they found that the platelets became nonuniformly distributed when the WSR was 440 s^{-1}. Although no study of lateral motion of platelet-sized particles in blood suspensions flowing at elevated WSR has visualized paths of individual particles, it is very likely that those paths are dominated by strong local interactions and hence resemble Goldsmith's records. Points of interest include whether the paths can in part be modelled by diffusion and what other concepts should enter into the model.

It is common to portray an individual particle in the shear flow of a suspension as interacting most strongly with its adjacent neighbors, which change due to the shear flow. The aspects of interacting with and changing neighbors are often separated so that models/analogies can be built about the kinetic theory of gases. Reflecting this focus, the tracked particle is said to have undergone "collisions" with the other suspended particles. Since no means is available to specify the individual positions of the neighbors (and all the other particles) in the flow, the model is constructed with probabilities. The usual models involve unbiased random walks, which excludes environments with force fields and nonuniform probabilities for interacting with neighbors. Many models of unbiased random walks translate directly to a diffusion equation.

Such models obscure viewpoints that focus on the lateral motion of individual particles and on the suspension as a complex fluid. Studies of flowing dilute suspensions show that particles can move laterally as they pass through a tube or channel. The lateral motion of individual particles is largest near the wall and deformable bodies exhibit much larger motions than similar rigid bodies. In part the lateral force is due to restriction of fluid motions by the wall. However, mathematical models of these events have linked the lateral forces to both the gradient and the curvature of the velocity profile in unbounded flows. In a practical sense, such forces

are also linked to the wall, since the no-flow boundary condition there leads to the overall velocity profile. Both experiments and theory show that the lateral force decreases greatly as the distance from the wall increases. These ideas blend naturally into a picture of the suspension as a complex fluid. The relative lack of particles near the wall can be ascribed to a combination of mechanical interference and lateral motion due to wall-related repulsive force. The net clearance of the wall region is limited in nondilute suspensions, because the shearing motion in the major portion of the suspension acts to return particles toward the wall. This balance of events leads to a lateral gradient of concentration of the red cells. Experiments that study this gradient usually focus on the extra suspending fluid (plasma) in the region, as reflected in the names, marginal and peripheral plasma layers. Examining the bead concentration profiles from either transient or steady-state experiments shows that the near-wall peak is located in this gradient of hematocrit. The peak of the bead profile is slightly further off the wall than would be predicted if simple mechanical interference were the only source of exclusion; this finding is consistent with flow-induced repulsion.

The mechanical behavior of red cells in flow (Goldsmith and Turitto, 1986; Schmid-Schoenbein and Wells, 1969; Chien, 1975) leads one to expect that the interaction with nearest neighbors changes with the WSR. At low shear rates, an isolated red cell tumbles like a solid; at intermediate shear rates, it exhibits drop-like deformation; and at high shear stresses, usually obtained by use of high-viscosity suspending fluid, the membrane has been observed to circulate (tank-treading). These behaviors are associated with the transfer of stress from the outer fluid across the membrane to the inner hemoglobin solution. Equally important, it has been shown that when the WSR is sufficient to deform red cells, the cells spend a greater fraction of their time aligned toward the flow direction than when they move on orbits, as rigid particles do. Transfer of stress occurs in both dilute and concentrated suspension flows, but the above associated effects, which are readily observed in dilute suspensions, are likely to be reduced and difficult to observe in concentrated blood suspensions. While both particle crowding, which leads to red cell deformation at even low shear rates, and random lateral motions will act to obscure the directed events found in dilute suspensions (e.g., alignment, tendency to migrate) (Goldsmith and Turitto, 1986), it seems reasonable to expect that such shear-induced effects are present at nondilute (normal) hematocrits.

Although direct visualization may not disclose such events, they may reveal themselves as a kind of average event, e.g., a drift. Improvements in the collisional model require accounting for the spatially varying lateral force and the nonuniform arrangement of neighbors, which are both likely to depend on the local shear rate. In a sense, improving the analogy involves finding a better random walk model. It is well known that random walks involving forces or nonuniform environments will exhibit drift, a convection-like behavior, as well as diffusive motion (Berg, 1993). As shown in a previous paper, random walks that include a special pattern of drifting motion will lead to nonuniform concentration profiles of a tracer species (Eckstein and Belgacem, 1991); the ideas there are a significant expansion of concepts discussed earlier (Eckstein, 1982).

The above discussion ignored development of the radial concentration profile of the major suspended species, the red cells, which probably occurs along the flow direction. This redistribution is associated with an axial variation of the lateral gradient of hematocrit. Further, as net amounts of red cells were displaced inward, there was an outward directed movement of suspending fluid; such a flow may have carried platelet-sized beads outward. One reason for neglecting such effects is that they would at most lead to a 2.5-fold increase in bead concentration; that amount is insufficient to explain the large near-wall excesses observed in steady-state tube flows. (This estimate is based on a total separation of red cells from the suspending fluid for a hematocrit of 40%; assumptions include packing all the red cells in the center of the tube and segregating all the beads and suspending fluid between the packed red cells and the tube wall.) Another reason is less direct; large near-wall excesses do not occur within the first diameter of tube length, where the most significant redistribution of red cells probably occurs because of the acceleration, deceleration, and radial velocity fields associated with establishing the shear stress profile. Last, after the basic marginal layer is established in the entrance region, the outward flow of suspending fluid must be relatively small near the wall because that region is already relatively rich in suspending fluid and any radial velocity field must decrease to 0 at the wall to satisfy the continuity equation. Despite these points, a case for studying axial changes of lateral red cell redistribution can be made because the shape of the radial hematocrit profile is unknown for diameters as large as those of these experiments and because the redistribution of red cells may act synergistically with other mechanisms.

Available volume model

Arguments based on theory and experimental data make it reasonable to reject a hypothetical model for the nondiffusive transport. The hypothesis was built on concepts from the theory of imperfect gases; it involved defining an *effective platelet concentration* as the ratio of the number of platelets to the available volume for platelets (Blackshear et al., 1977). To build an appreciation for the concept of available volume, consider a space bounded by walls and/or defined planes; the space already contains particles. The volume remaining in the space can be separated into two portions: 1) the excluded volume, which is composed of regions at the boundary of each particle already in the space and a region next to any wall bounding the space; and 2) the available volume, which is what is left after the excluded volume is deducted from the remaining volume. The excluded volume is that space next to a surface (of a particle or wall) where the center of another particle cannot be located because of mechanical interference. For suspension flows, the commonly cited example of

"excluded volume" involves the zone of lower concentration immediately adjacent the wall, often termed a Vand zone.

The available and excluded volumes in the model were hypothesized to depend on the shear rate (Blackshear et al., 1977) because shear flow disrupts rouleaux, which have a lesser amount of exposed surface than dispersed red cells. At low shear rates, rouleaux would form and would consume a relatively small portion of the total space as excluded volume. At higher shear rates, more red cells would be independently suspended and the amount of excluded volume would increase. A calculation based on theory that is applicable to dilute situations showed that no available volume would remain in a 40% hematocrit suspension if all the red cells were surrounded by a layer of excluded volume with a thickness equal to the radius of a platelet (Blackshear et al., 1977). Such a situation was expected to occur when the local shear broke up all the rouleaux. Then, as the available volume approached zero, the local *effective platelet concentration* would rise immensely, leading to a massive concentration gradient that would drive the flux of platelets toward the wall. Sufficient available volume was expected to remain near the wall because of the mechanical exclusion of red cells by the wall and the relatively larger flow-induced lateral force on flexible bodies.

If the above hypothesis were correct, experiments at hematocrits of 40% and above should have produced concentration profiles that had regions with near-zero values of concentration. This was not observed, nor were large near-wall excesses of beads found in steady-state trials that used suspensions with 60 and 80% hematocrit, conditions for which large near-wall excesses would have been expected if the calculation were inaccurate. The significant near-wall peaks observed in profiles from experiments with 15% hematocrit indicate that nondiffusive modes of lateral transport occur independently of available volume effects.

Further reason to doubt the entire hypothesis is provided by considering methods to calculate the excluded volume for nondilute conditions. In a dilute situation it is reasonable to place a region of excluded volume around each red cell, but as Tanford (1961) notes, in nondilute situations, the calculation involves conditional probabilities that reflect the many possible closely spaced arrangements of particles that were previously placed. In particular, Tanford provides an illustration of two particles that are sufficiently close together so the excluded volume surrounds the pair, and as a result, is less than the sum of excluded volumes for two particles that are relatively far apart. For such reasons, it is doubtful that greatly increasing amounts of excluded volume in sheared red cells suspensions will accompany increases in the hematocrit. Also, for a suspension of two different species, the calculation must consider entropic effects associated with placing all red cells before any platelets; this is another reason for the use of conditional probabilities. These and other arguments based on theory indicate that available volume will not decrease dramatically over a small range of hematocrit. Overall, it seems reasonable to reject the hypothesis since it does not provide a way to order the experimental data and since the theoretical calculations become forbiddingly complex.

Further treatment of this data

This paper describes experiments that concretely demonstrate the nature of events related to transient anomalous lateral transport of platelet-sized objects in flowing red cell suspensions. Two papers are being prepared that relate to the data presented here for the parameters of 40% hematocrit and 560 s^{-1} WSR. One presents an estimate of the shape function that describes of the drift motion in a previously published model of the lateral transport (Eckstein and Belgacem, 1991). The other paper uses that shape function in simulations of the transient experiments and estimates an effective diffusion coefficient by matching simulated profiles to the experimental profiles shown above. The degree of match between the shape of the simulated and experimentally determined profiles will provide a way to evaluate the quality of the model.

CONCLUSIONS

Profiles observed in circumstances of transient lateral transport had features that indicated that a nondiffusive mode of transport occurred for hematocrits of 15 and 40% with WSR of ~550 s^{-1}. Larger amounts of lateral transport occurred in suspension flows with 40% hematocrit than with 15% hematocrit. Flows with WSRs of 520 to 1220 s^{-1} had larger amounts of lateral transport than flows with a WSR of 250 s^{-1}; for the larger WSR, the amount of lateral transport appears to be proportional to the WSR.

We thank Dr. Elizabeth A. Tolley of the Division of Epidemiology and Biostatistics at the University of Tennessee, Memphis, for expert advice on statistical methods. Ms. Anne Calvez discovered an error related to the measurement of tube diameters and corrected the error by reprocessing many images and recompiling the data and graphs; we greatly appreciate her help and fine critical skills.

This work was supported by the National Heart, Lung and Blood Institute through Grant HL-33100.

REFERENCES

Berg, H. C. 1993. Random Walks in Biology. Expanded edition. Princeton University Press, Princeton, NJ.

Bilsker, D. L., C. M. Waters, J. S. Kippenhan, and E. C. Eckstein. 1989. A freeze-capture method for the study of platelet-sized particle distributions. *Biorheology*. 26:1031–1040.

Blackshear, P. L., K. W. Bartelt, and R. J. Forstrom. 1977. Fluid dynamic factors affecting particle capture and retention, *Ann. N.Y. Acad. Sci.* 283: 270–279

Chien, S. 1975. Biophysical behavior of red cells in suspensions. *In* The Red Blood Cell. Vol II. D. Surgenor and N. Mac, editors. Academic Press, New York. 1032–1135.

Corattiyl, V., and E. C. Eckstein. 1986. Regional platelet concentration in bloodflow through capillary tubes. *Microvasc. Res.* 33:261–270.

Eckstein, E. C. 1982. Rheophoresis—a broader concept of platelet dispersivity. *Biorheology*. 19:717–724.

Eckstein, E. C., and F. Belgacem. 1991. Model of platelet transport in flowing blood with drift and diffusion terms. *Biophys. J.* 60:53–69.

Eckstein, E. C., J. F. Koleski, and C. M. Waters. 1989. Concentration profiles of 1 and 2:5 μm beads during blood flow: hematocrit effects. *Trans. Am. Soc. Artif. Intern. Organs.* 35:188–190.

Eckstein, E. C., A. W. Tilles, and F. J. Millero. 1988. Conditions for the occurrence of large near-wall excesses of small particles during blood flow. *Microvasc. Res.* 36:31–39.

Goldsmith, H. L. 1971. Red cell motions and wall interactions in tube flow. *Fed. Proc.* 30:1578–1588.

Goldsmith, H. L., and V. T. Turitto. 1986. Rheological aspects of thrombosis and haemostasis: basic principles and applications. *Thromb. Haemost.* 55:415–435.

Kippenhan, J. S. 1987. Computer methods for estimating concentration profiles of platelet-sized particles in blood suspensions. M.S. thesis. University of Miami, Coral Gables, FL.

Probstein, R. F. 1989. Physicochemical Hydrodynamics: An Introduction. Butterworths, Stoneham, MA.

Schmid-Schoenbein, H., and R. Wells. 1969. Fluid drop-like transition of erythrocytes under shear. *Science.* 165:288–291.

Silverman, B. W. 1986. Density Estimation for Statistics and Data Analysis. Chapman and Hall, New York.

Tanford, C. 1961. Physical Chemistry of Macromolecules. John Wiley & Sons, New York. 192–196.

Tilles, A. W., and E. C. Eckstein. 1987. The near-wall excess of platelet-sized particles in blood flow: its dependence on hematocrit and wall shear rate. *Microvasc. Res.* 33:211–223.

Turitto, V. T., A. M. Benis, and E. F. Leonard. 1972. Platelet diffusion in flowing blood. *Ind. Eng. Chem. Fundam.* 11:216–233.

Waters, C. M., and E. C. Eckstein. 1990. Concentration profiles of platelet-sized latex beads for conditions relevant to hollow-fiber hemodialyzers. *Artif. Organs.* 14:7–13.

Yeh, C. 1991. Direct demonstration of a radial drift of platelet-sized latex beads in flows of blood suspension. M. S. Thesis, University of Miami, Coral Gables, FL.